First observation of the $K^+ \to \pi^+\nu\bar{\nu}$ decay with the NA62 experiment

Ilaria Rosa *on behalf of the NA62 Collaboration* (*)
Scuola Superiore Meridionale e INFN, Sezione di Napoli, I-80138 Napoli, Italy

Summary. — The NA62 experiment at CERN is designed to study the $K^+ \to \pi^+\nu\bar{\nu}$ decay. After collecting data in 2016, 2017, and 2018, the experiment resumed data taking in 2021 and has received approval for operations until the start of Long Shutdown 3 in 2026. The first observation of the $K^+ \to \pi^+\nu\bar{\nu}$ decay achieved combining the data collected in 2016-2022 is reported.

(*) The NA62 Collaboration: A. Akmete, R. Aliberti, F. Ambrosino, R. Ammendola, B. Angelucci, A. Antonelli, G. Anzivino, R. Arcidiacono, M. U. Ashraf, T. Bache, A. Baeva, D. Baigarashev, L. Bandiera, M. Barbanera, V. Bautin, J. Bernhard, A. Biagioni, L. Bician, C. Biino, A. Bizzeti, T. Blazek, B. Bloch-Devaux, P. Boboc, V. Bonaiuto, M. Boretto, M. Bragadireanu, A. Briano Olvera, D. Britton, F. Brizioli, M.B. Brunetti, D. Bryman, F. Bucci, N. Canale, T. Capussela, J. Carmignani, A. Ceccucci, P. Cenci, M. Ceoletta, V. Cerny, C. Cerri, X. Chang, B. Checcucci, A. Conovaloff, P. Cooper, E. Cortina Gil, M. Corvino, F. Costantini, A. Cotta Ramusino, D. Coward, P. Cretaro, G. D'Agostini, J.B. Dainton, P. Dalpiaz, H. Danielsson, B. De Martino, M. D'Errico, N. De Simone, D. Di Filippo, L. Di Lella, N. Doble, B. Dobrich, F. Duval, V. Duk, D. Emelyanov, J. Engelfried, T. Enik, N. Estrada-Tristan, V. Falaleev, R. Fantechi, V. Fascianelli, L. Federici, S. Fedotov, A. Filippi, R. Fiorenza, M. Fiorini, M. Francesconi, O. Frezza, J. Fry, J. Fu, A. Fucci, L. Fulton, E. Gamberini, L. Gatignon, G. Georgiev, S. Ghinescu, A. Gianoli, R. Giordano, M. Giorgi, S. Giudici, F. Gonnella, K. Gorshanov, E. Goudzovski, C. Graham, R. Guida, E. Gushchin, F. Hahn, H. Heath, J. Henshaw, Z. Hives, E.B. Holzer, T. Husek, O. Hutanu, D. Hutchcroft, L. Iacobuzio, E. Iacopini, E. Imbergamo, B. Jenninger, J. Jerhot, R.W. Jones, K. Kampf, V. Kekelidze, C. Kenworthy, D. Kereibay, S. Kholodenko, G. Khoriauli, A. Khotyantsev, A. Kleimenova, M. Kolesar, A. Korotkova, M. Koval, V. Kozhuharov, Z. Kucerova, Y. Kudenko, J. Kunze, V. Kurochka, V. Kurshetsov, G. Lanfranchi, G. Lamanna, E. Lari, G. Latino, P. Laycock, C. Lazzeroni, G. Lehmann Miotto, M. Lenti, E. Leonardi, S. Lezki, P. Lichard, L. Litov, P. Lo Chiatto, R. Lollini, D. Lomidze, A. Lonardo, P. Lubrano, M. Lupi, N. Lurkin, D. Madigozhin, I. Mannelli, A. Mapelli, F. Marchetto, R. Marchevski, S. Martellotti, P. Massarotti,K. Massri, E. Maurice, M. Medvedeva, A. Mefodev, E. Menichetti, E. Migliore, E. Minucci, M. Mirra, M. Misheva, N.Molokanova, M. Moulson, S. Movchan, Y. Mukhamejanov, A. Mukhamejanova, M. Napolitano, R. Negrello, I. Neri, F. Newson, A. Norton, M. Noy, T. Numao, V. Obraztsov, A. Okhotnikov, A. Ostankov, S. Padolski, R. Page, V. Palladino, I. Panichi, A. Parenti, C. Parkinson, E. Pedreschi, M. Pepe, M. Perrin-Terrin, L. Peruzzo, L. Petit, P. Petrov, Y. Petrov, F. Petrucci, R. Piandani, M. Piccini, J. Pinzino, I. Polenkevich, C. Polivka, L. Pontisso, Yu. Potrebenikov, D. Protopopescu, M. Raggi, M. Reyes Santos, K. Rodriguez Rivera, M. Romagnoni, A. Romano, I. Rosa, P. Rubin, G. Ruggiero, V. Ryjov, A. Sadovsky, N. Saduyev, S. Sakhiyev,K.Salamatin, A. Salamon, C.Sam, J.Sanders, C. Santoni, G. Saracino, F.Sargeni, J. Schubert, S. Schuch- mann, V. Semenov, A. Sergi, A. Shaikhiev, S. Shkarovskiy, M. Soldani, D. Soldi, M. Sozzi, T. Spadaro, F. Spinella, A. Sturgess, V. Sugonyaev, J. Swallow, A. Sytov, G. Tinti, A. Tomczak, S. Trilov, M. Turisini, P. Valente, T. Velas, B. Velghe, S. Venditti, P. Vicini, R. Volpe, M. Vormstein, H. Wahl, R. Wanke, V. Wong, B. Wrona, O. Yushchenko, M.Zamkovsky, A. Zinchenko.

1. – Introduction

NA62 at CERN is a fixed-target experiment designed to measure the $K^+ \to \pi^+\nu\bar{\nu}$ branching fraction. The layout of the NA62 beamline and detector is described in [1].

The NA62 experiment, thanks to the versatility of the experimental setup, combined with the multiple trigger chains available [2], is able to investigate a variety of K^+ meson decays, including lepton flavour and lepton number violating decays, precision measurements, and searches for long-lived particles in leptonic and hadronic final states [3, 4, 5, 6, 7, 8, 9, 10].

During the Long Shutdown 2 (LS2), NA62 underwent crucial detector upgrades and resumed data taking in 2021. The analysis of the data collected in the 2016–2018 run provided 3σ evidence for the $K^+ \to \pi^+\nu\bar{\nu}$ decay [11]. In this contribution, the first observation of the $K^+ \to \pi^+\nu\bar{\nu}$ decay using the data collected in 2021–2022 is reported, together with the combination with previous results.

2. – The NA62 detector

NA62 is located in the North Area at the CERN SPS. Charged kaons pass through the NA62 experiment as part of a secondary hadron beam derived from interactions of protons from the SPS with a beryllium target. The secondary beam is defined to have a momentum of 75 GeV, and is mostly composed of pions and protons, with kaons making up about 6% of the beam. A fraction of the K^+ decays in flight within a 60 m long fiducial volume (FV).

Before entering a large vacuum tank, each K^+ is identified, time-stamped, and has its momentum reconstructed using a silicon-pixel detector (GTK) and a differential Cherenkov detector (KTAG). An upstream veto system consisting of the veto counter (VC), CHANTI, and ANTI0 detectors, detects particles from upstream K^+ decays or interactions. After the fiducial volume, a STRAW spectrometer measures the momentum of the products of kaons decaying in the FV with a precision of about 0.3%. Photon veto detectors, including large-angle vetoes (LAV), a liquid krypton calorimeter (LKr), two hadronic calorimeters (MUV1-2), a intermediate-ring and a small-angle calorimeters (IRC, SAC), suppress events containing photons with an inefficiency below 10^{-8}. A RICH identifies charged particles in the momentum range relevant for kaon decays and provides the trigger reference time. The MUV3 detector provides additional muon identification information, together with the MUV1-2, and contributes to the level-0 trigger system.

3. – The $K^+ \to \pi^+\nu\bar{\nu}$ decay

The $K^+ \to \pi^+\nu\bar{\nu}$ decay is a flavour-changing neutral current (FCNC) process. In the Standard Model (SM), it proceeds through electroweak box and penguin diagrams, dominated by short-distance contributions involving virtual top quark exchange. The decay is highly suppressed due to the GIM mechanism and the CKM suppression of the $t \to d$ transition. The $K^+ \to \pi^+\nu\bar{\nu}$ branching ratio can be predicted within the SM using different inputs for the CKM matrix elements. Using tree-level determinations of the CKM parameters, the predicted value is $\mathcal{B}(K^+ \to \pi^+\nu\bar{\nu}) = (8.4 \pm 1.0) \times 10^{-11}$ [12]. When inputs from meson mixing observables are used, a branching ratio $(8.60 \pm 0.42) \times 10^{-11}$ is predicted [13].

The $K^+ \to \pi^+\nu\bar{\nu}$ decay is sensitive to a variety of effects of physics beyond the SM (BSM), probing new physics at mass scales up to $\mathcal{O}(100$ TeV) [14]. Different BSM scenarios predict significant deviations of the branching ratio from the SM prediction, as well as correlations with other flavour observables and the $K_L \to \pi^0\nu\bar{\nu}$ decay [15, 16, 17].

4. – Data sample and selection

The data used in this analysis were collected by the NA62 experiment in 2021 and 2022 at the nominal beam intensity of 580 MHz. Events were selected using three dedicated trigger lines: MB for $K^+ \to \mu^+\nu$ control samples, NORM for $K^+ \to \pi^+\pi^0$ decays used for normalisation, and PNN for $K^+ \to \pi^+\nu\bar{\nu}$ signal candidates.

A beam K^+ is tagged by the KTAG and its momentum measured by the GTK. A single downstream π^+ track is reconstructed in the STRAW and identified using RICH, LKr, and MUVs information. A BDT classifier combining informations from the calorimeter and muon veto detectors is used for particle identification. The pion momentum is required to be between 15 and 45 GeV/c, with no associated MUV3 signal.

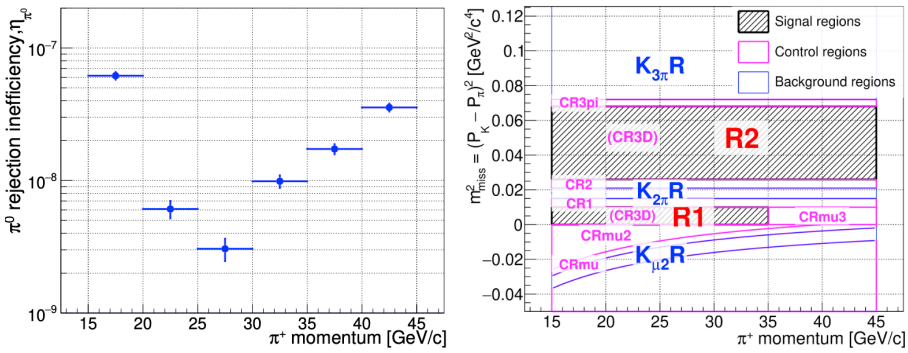

Fig. 1. – Left: π^0 rejection inefficiency as a function of the π^+ momentum. Right: definitions of kinematic regions in the (p_{π^+}, m^2_{miss}) plane. Region CR3D is the same as the signal region in this projection, but contains events outside the 3-dimensional signal regions definition.

The kaon and pion tracks are matched in space and time, requiring a common vertex within the FV and a closest distance of approach below 4 mm. Upstream activity is suppressed using vetoes from the GTK, VC, CHANTI, and ANTI0 detectors, together with a BDT trained to reject such backgrounds.

Photon vetoes are applied using LAV, LKr, IRC, and SAC detectors, and multiplicity vetoes reject events with additional activity in CHOD, NA48-CHOD, MUV0, and STRAW. Kinematic regions are defined using the squared missing mass, $m^2_{\rm miss} = (P_K - P_\pi)^2$, and the pion momentum p_{π^+}, with P_K and P_π reconstructed from GTK and STRAW measurements, respectively.

Background regions are defined around the main kaon decay modes: $K^+ \to \mu^+\nu$, $K^+ \to \pi^+\pi^0$, and $K^+ \to \pi^+\pi^+\pi^-$. Control regions are used to validate the background estimation and to evaluate the kaon flux while signal events are required to lie within R1 or R2 (Fig: 1).

5. – Single event sensitivity

The branching ratio of $K^+ \to \pi^+\nu\bar{\nu}$ is measured relatively to the $K^+ \to \pi^+\pi^0$ decay. The selection of the normalisation $K^+ \to \pi^+\pi^0, \pi^0 \to \gamma\gamma$ channel relies only on charged particles and largely overlaps with the signal selection.

The effective number of K^+ decays is computed as:

$$N_K = \frac{N_{\pi\pi}^{\text{eff}} \cdot D}{\mathcal{B}_{\pi\pi} \cdot A_{\pi\pi}}, \tag{1}$$

where $N_{\pi\pi}^{\text{eff}}$ is the background-subtracted number of normalisation events, $\mathcal{B}_{\pi\pi}$ is the branching ratio of the normalisation $K^+ \to \pi^+\pi^0, \pi^0 \to \gamma\gamma$ decay chain, $A_{\pi\pi}$ is the acceptance for the normalisation selection and D is the downscaling factor of the NORM trigger line ($D = 400$).

The single event sensitivity (SES) is defined as the branching ratio corresponding to one expected signal event:

$$\mathcal{B}_{\text{SES}} = \frac{1}{N_K \cdot A_{\pi\nu\bar{\nu}} \cdot \varepsilon_{\text{trig}} \cdot \varepsilon_{\text{RV}}}, \tag{2}$$

where $A_{\pi\nu\bar{\nu}}$ is the signal acceptance, $\varepsilon_{\text{trig}}$ is the ratio of trigger efficiencies between the PNN and NORM triggers and ε_{RV} is the random veto efficiency.

The analysis is performed in six bins of p_{π^+} between 15 and 45 GeV/c. In each bin p_i, the expected number of signal events assuming a given SM branching ratio $\mathcal{B}_{\pi\nu\bar{\nu}}^{\text{SM}}$ is estimated as:

$$N_{\pi\nu\bar{\nu}}^{\text{SM}}(p_i) = \mathcal{B}_{\pi\nu\bar{\nu}}^{\text{SM}} \cdot \frac{N_{\pi\pi}^{\text{eff}}(p_i) \cdot D}{\mathcal{B}_{\pi\pi} \cdot A_{\pi\pi}(p_i)} \cdot A_{\pi\nu\bar{\nu}}(p_i) \cdot \varepsilon_{\text{trig}}(p_i) \cdot \varepsilon_{\text{RV}}(p_i). \tag{3}$$

In the 2022 dataset, the average expected number of SM signal events per SPS spill is 2.5×10^{-5}, compared to 1.7×10^{-5} in the 2018 data. The corresponding single event sensitivity is $(8.5 \pm 0.3) \times 10^{-12}$, where the dominant contribution to the uncertainty comes from the estimation of the acceptances ratio.

6. – Background estimation

Backgrounds to the $K^+ \to \pi^+\nu\bar{\nu}$ signal arise from both the main kaon decay modes and upstream decays or interactions. The background estimation is performed using both data-driven methods and Monte Carlo (MC) simulations.

The $K^+ \to \mu^+\nu$, $K^+ \to \pi^+\pi^0$, and $K^+ \to \pi^+\pi^+\pi^-$ decays can enter in the signal regions via the non-Gaussian tails of the m_{miss}^2 distribution. For each channel, the number of events in the respective background region of the $(p_{\pi^+}, m_{\text{miss}}^2)$ plane is extrapolated to the signal regions using control samples. Corrections are applied for specific radiative decays, such as $K^+ \to \mu^+\nu\gamma$ and $K^+ \to \pi^+\pi^0\gamma$, which are not fully captured in the control regions.

The $K^+ \to \pi^+\pi^0(\gamma)$ background is suppressed through a combination of kinematic selection and photon vetoes, assumed to factorize. The modeling of the m_{miss}^2 distribution is based on a sample where the π^0 is tagged independently. MC simulations are used to correct for small correlations due to radiative photons.

The estimation of $K^+ \to \mu^+\nu(\gamma)$ relies on calorimetric and RICH-based muon identification. When a photon overlaps with a high-energy muon ($E_\mu > 30$ GeV), both kinematics and particle identification degrade. A dedicated control sample, selected by requiring a MUV3 signal and enhanced muon-photon overlap, is used to model this background.

Minor backgrounds such as $K^+ \to \pi^+\gamma\gamma$ and $K^+ \to \pi^- e^+ \nu$ are estimated from MC and found to be negligible.

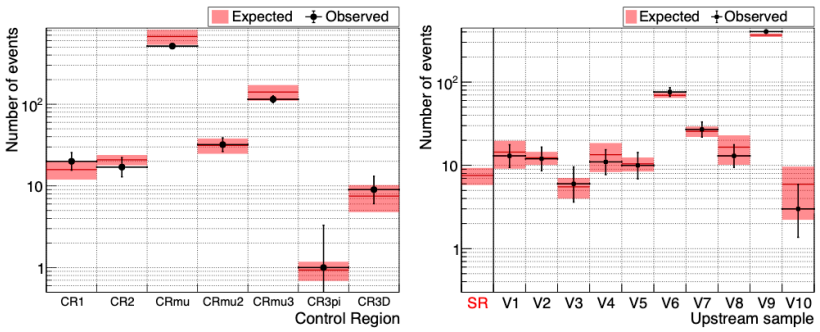

Fig. 2. – Left: expectations and observations in control regions. Right: expectations and observations in upstream background validation samples.

The upstream background arises from kaon decays and interactions occurring upstream of the fiducial volume, where a downstream π^+ is incorrectly associated with an unrelated GTK track, resulting in a fake reconstructed vertex. It is estimated using a fully data-driven method based on a control sample selected with inverted kaon–pion matching, weighted by the measured mismatching probability. Dedicated upstream-enriched control samples are used to validate the procedure.

The total background expectation for the 2021–2022 dataset, integrated over pion momentum, is $11.0^{+2.1}_{-1.9}$. The validation of the background estimates in control and upstream-enriched regions is shown in Figure 2.

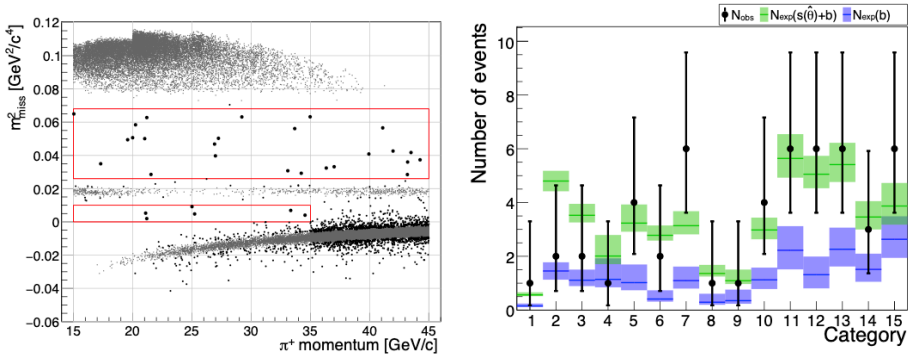

Fig. 3. – Left: distribution of events satisfying the signal selection in the $(p_{\pi^+}, m^2_{\rm miss})$ plane. Right: numbers of expected and observed events in the categories used for the statistical analysis of 2016–2022 data. Blue and green represent background and total (measured signal plus background) expectation, respectively.

7. – Results

After applying the signal selection on the 2021-2022 dataset, 31 events remain in the signal regions, as shown in Fig.3-left.

Performing a profile likelihood ratio test statistic in the six π^+ momentum bins, the analysis of 2021–2022 data results in the measurement

$$\mathcal{B}(K^+ \to \pi^+ \nu\bar{\nu}) = \left(16^{+4.0}_{-4.2}\big|_{\text{stat}}\,{}^{+1.4}_{-1.3}\big|_{\text{syst}}\right) \times 10^{-11}.$$

The combination of the 2016–18 and 21–22 results is obtained by grouping the 2016–18 data into nine categories. The p-value of the background-only hypothesis is found to be 2×10^7 leading, for the first time, to a rejection of the background-only hypothesis with a significance above 5σ.

The branching ratio measured from the fit to the combined dataset is

$$\mathcal{B}(K^+ \to \pi^+ \nu\bar{\nu}) = \left(13.0^{+3.0}_{-2.7}\big|_{\text{stat}} \pm 1.3_{\text{syst}}\right) \times 10^{-11} = \left(13.0^{+3.3}_{-3.0}\right) \times 10^{-11}.$$

8. – Conclusion

The NA62 experiment has observed the decay $K^+ \to \pi^+ \nu\bar{\nu}$ with a significance greater than 5σ. The measured branching ratio is $\mathcal{B}(K^+ \to \pi^+ \nu\bar{\nu}) = \left(13.0^{+3.3}_{-3.0}\right) \times 10^{-11}$, representing the smallest branching ratio measured with a significance above 5σ. The relative uncertainty of the measurement is 25%, dominated by statistical uncertainties. The measurement [18] is consistent across data-taking periods and is compatible with the results from the BNL E787 and E949 experiments [19]. The central value is compatible within 1.5–1.7σ with respect to the standard model predictions.

In 2023 and 2024, NA62 collected a dataset with similar statistics to that of the 2016–2022 period. An additional dataset of comparable size is expected from the 2025–2026 runs. With the full dataset, NA62 aims to reduce the relative uncertainty on the branching ratio measurement to below 20%.

REFERENCES

[1] NA62 collaboration, *JINST*, **12** (2017) P05025
[2] NA62 collaboration, *JHEP*, **03** (2023) 122
[3] NA62 collaboration, *JHEP*, **09** (2023) 040
[4] NA62 collaboration, *Phys. Lett. B*, **846** (2023) 138193
[5] NA62 collaboration, *JHEP*, **11** (2022) 011
[6] NA62 collaboration, *Phys. Lett. B*, **838** (2023) 137679
[7] NA62 collaboration, *Phys. Lett. B*, **859** (2024) 139122
[8] NA62 collaboration, *JHEP*, **09** (2023) 035
[9] NA62 collaboration, *Phys. Rev. Lett.*, **133** (2024) 111802
[10] NA62 collaboration, *Eur. Phys. J. C*, **85** (2025) 1133
[11] NA62 collaboration, *JHEP*, **06** (2021) 093
[12] G. D'Ambrosio, A.M. Iyer, F. Mahmoudi, S. Neshatpour, *JHEP*, **09** (2022) 148.
[13] A.J. Buras, E. Venturini, *Eur. Phys. J. C*, **82** (2022) 615
[14] A.J. Buras, D. Buttazzo, J. Girrbach-Noe, R. Knegjens, *JHEP*, **11** (2015) 033.
[15] C. Bobeth, A.J. Buras, A. Celis, M. Jung, *JHEP*, **04** (2017) 079.
[16] M. Bordone, D. Buttazzo, G. Isidori, J. Monnard, *Eur. Phys. J. C*, **77** (2017) 618.
[17] A.J. Buras, J. Harz, M.A. Mojahed, *JHEP*, **10** (2024) 087.

[18] The NA62 collaboration, Cortina Gil *et al.*, *JHEP*, **02** (2025) 191.
[19] BNL-E949 collaboration, A.V. Artamonov *et al.*, *Phys. Rev. D*, **79** (2009) 092004